ELSEVIER

Journal of Alloys and Compounds 408–412 (2006) 1267–1273

Journal of ALLOYS AND COMPOUNDS

www.elsevier.com/locate/jallcom

Electrochemical behavior of actinides and actinide nitrides in LiCl–KCl eutectic melts

Osamu Shirai [a,*], Hajimu Yamana [a], Yasuo Arai [b]

[a] *Research Reactor Institute, Kyoto University, Asashiro-nishi 2-1010, Kumatori-cho, Sennan-gun, Osaka 590-0494, Japan*
[b] *Department of Nuclear Energy System, Japan Atomic Energy Research Institute, Oarai-machi, Higashi-ibaraki, Ibaraki 311-1394, Japan*

Available online 6 June 2005

Abstract

The redox potentials of the U^{3+}/U, Np^{3+}/Np and Pu^{3+}/Pu couples at Mo, Cd and Bi electrodes in LiCl–KCl eutectic melt containing UCl_3, $NpCl_3$ and $PuCl_3$, respectively, were evaluated by electrochemical measurements at the temperature range between 723 and 823 K. The standard potentials of the U^{3+}/U, Np^{3+}/Np and Pu^{3+}/Pu couples versus the Ag^+/Ag (1 wt.% AgCl) reference electrode were given by the following equations: $E^0_{U^{3+}/U} = -1.8647 + 0.000798 \times T$, $E^0_{Np^{3+}/Np} = -2.0298 + 0.000706 \times T$ and $E^0_{Pu^{3+}/Pu} = -2.232 + 0.00094 \times T$, where E values are in volts, T in kelvin. The differences between the redox potentials at Mo electrode and those at liquid metal electrodes were attributable to the lowering in the activities of U, Pu and Np in liquid metal phases according to the alloy formation. Similarly, the anodic dissolutions of UN, NpN and PuN were observed at about 0.7 V more positive potential than those of U, Np and Pu, respectively, since the stabilization of U, Np and Pu by nitriding lowered the activities of U, Np and Pu, respectively, in the solid phase.

Keywords: Voltammetry; Uranium; Neptunium; Plutonium; Nitride fuel

1. Introduction

Japan Atomic Energy Research Institute (JAERI) has proposed the double-strata fuel cycle for transmutation of long-lived minor actinides (MAs) [1]. The transmutation system proposed by JAERI is a Pb–Bi cooled sub-critical accelerator driven system with ^{15}N-enriched MAs nitride fuels. Actinide nitrides have been chosen as candidate materials of advanced fuels and targets for fast reactors and for transmutation of MAs because the thermal conductivity and metal density are higher than those of actinide oxides and it has high melting temperature [2–4]. Besides above advantages, the mutual miscibility among the actinide nitrides is prospected since their crystal structures are identical with similar lattice constants [2]. However, the recycling of ^{15}N-enriched nitrogen, which is used for depression of the formation of ^{14}C, is required in the reprocessing of nitride fuel [5]. As for the reprocessing, the aqueous process such as PUREX is not adequate for nitride fuel with ^{15}N-enriched nitrogen, because it will be diluted and dispersed by the isotopic exchange in nitric acid. Then, the application of the pyrochemical reprocessing to nitride fuel cycle has been proposed since ^{15}N can be easily recovered and the introduction of the pyrochemical process will realize more compact facilities [6,7].

In order to apply the pyrochemical reprocessing to nitride fuel cycle, the authors have investigated the individual electrode reaction of actinide nitrides such as UN, PuN and NpN in the LiCl–KCl eutectic melt [8–10]. In the electrorefining process, spent fuels are anodically dissolved in LiCl–KCl eutectic melt, and U, Pu and MAs are recovered together at the cathode. It has been proposed that U could be selectively recovered at the solid cathode due to the difference in the formation energies of chlorides, and Pu and MAs at the liquid metal cathode due to their small activity coefficients in the liquid metals such as Cd or Bi [11,12]. Cd and Bi are assumed to be typical liquid metals, since Cd and Bi have low melting points and the activities of lanthanides and actinides in their liquid phases are very small. Therefore, it is necessary

* Corresponding author. Tel.: +81 724 51 2424; fax: +81 724 51 2634.
E-mail address: shirai@hl.rri.kyoto-u.ac.jp (O. Shirai).

0925-8388/$ – see front matter © 2005 Elsevier B.V. All rights reserved.
doi:10.1016/j.jallcom.2005.04.119

to elucidate the electrode reaction of U, Pu and MAs at the liquid Cd and Bi electrodes.

In the present paper, recent studies on the redox reaction of actinides (An) such as the U^{3+}/U, Np^{3+}/Np and Pu^{3+}/Pu couples and/or lanthanides (Ln) such as the La^{3+}/La and Ce^{3+}/Ce couples at the solid and liquid metal electrodes and on the electrochemical behaviors of actinide nitrides (UN, NpN and PuN) in LiCl–KCl molten salts are summarized.

2. Experimental

The electrochemical cell used for the studies on the redox reaction of the U^{3+}/U, Np^{3+}/Np, Pu^{3+}/Pu, La^{3+}/La and Ce^{3+}/Ce couples at the solid or liquid metal electrodes was previously shown [13]. A Mo wire of 1.0 mm diameter also served as a working electrode. The Mo wire was encased in a high-purity alumina tube in such a way that the apparent surface area of 0.332 cm^2 was exposed to the molten salt. Liquid Cd and Bi electrodes, used as working electrodes, were prepared as follows; some granules of Cd (99.999%; Soekawa Chemicals Co. Ltd.) and of Bi (99.99%; Soekawa Chemicals Co. Ltd.) were placed in separate crucibles made of high-purity aluminum nitride (99.6% AlN; Nikkato Co.). The crucibles were immersed in the LiCl–KCl melt phase. A Mo wire (>99.95%; Soekawa Chemicals Co. Ltd.) of 1.0 mm diameter sheathed with a high-purity alumina tube of 1.0 mm inner diameter and 2.0 mm outer diameter was then immersed in the liquid metal phase to be used as a lead wire. The surface area of the liquid metal electrode was 0.605 cm^2, ignoring the distortion of the liquid metal surface due to the surface tension and wetting of the surface of the crucible. A silver–silver chloride (Ag^+/Ag) electrode served as a reference electrode. The reference electrode consisted of a closed-end porous mullite tube (50% Al_2O_3 + 46% SiO_2; Nikkato Co.), in which the LiCl–KCl eutectic salt containing 1.00 wt.% AgCl was placed, and an Ag wire of 1.0 mm diameter was immersed in the salt. A carbon rod (99.998%; Tokai Carbon Co. Ltd.) of 3.0 mm diameter sheathed with a high-purity alumina tube of 3.0 mm inner diameter and 5.0 mm outer diameter was used as a counter electrode. The surface area of the carbon counter electrode in contact with the salt phase was about 6.5 cm^2.

The electrochemical cell used for the studies on the anodic dissolution of UN, NpN and PuN was previously shown [8]. A Mo net cage (o.d.: about 10 mmϕ, depth: about 12 mm, 1 mm mesh) was used as a working electrode, and one UN, NpN, or PuN pellet of 9.5 ± 0.5 mm in diameter and 3.5 ± 0.5 mm in thick was placed in the cage. The counter electrode used was a Mo wire of 1 mmϕ in diameter. The W cage and Mo electrodes were polished with emery clothes, and washed with 1 M HNO_3 and water. The reference Ag^+/Ag electrode used was the same as mentioned above.

The polarographic-grade LiCl–KCl eutectic salt, $LaCl_3$ (99.99%), $CeCl_3$ (99.99%) and $CdCl_2$ (>99.99%) were purchased from Aldrich-APL, Ltd. By reacting $CdCl_2$ in the LiCl–KCl eutectic melts with U, Np and Pu in the molten Cd phases at 773 K, the salts containing about 20 wt.% UCl_3, $NpCl_3$ and $PuCl_3$, respectively, were prepared [13]. These salts were added to the respective LiCl–KCl eutectic melts in order to adjust the concentration of UCl_3, $NpCl_3$ and $PuCl_3$ for the measurements. Temperatures of the salt phases were measured by a calibrated Chromel–Alumel thermocouple. Cyclic voltammograms were obtained using a voltammetric analyzer, Potentiostat/Galvanostat Model 273A (Seiko EG&G). The concentrations of $LaCl_3$, $CeCl_3$, UCl_3, $NpCl_3$ and $PuCl_3$ in the LiCl–KCl eutectic salts were determined by ICP-AES.

The sample preparation and electrochemical measurements were carried out in a glovebox with high-purity argon gas atmosphere (H_2O, O_2 < 2.0 ppm).

3. Results and discussion

3.1. The redox reactions of the U^{3+}/U, Np^{3+}/Np, Pu^{3+}/Pu, La^{3+}/La and Ce^{3+}/Ce couples at the solid electrodes

Fig. 1 shows a typical cyclic voltammograms obtained at the Mo electrode at 723 K at a potential scanning rate of 0.01 V s^{-1} when the mole fractions of UCl_3, $NpCl_3$, $PuCl_3$, $LaCl_3$ and $CeCl_3$ in LiCl–KCl eutectic salts were 0.00088, 0.00070, 0.0014, 0.00275 and 0.00273, respectively. There exists a linear relationship between the cathodic peak currents and the square roots of the potential scanning rate in the region between 0.01 and 0.2 V s^{-1}. The peak heights were approximately proportional to the concentrations of the An^{3+} and Ln^{3+}. The cathodic and the anodic peaks correspond to a redox couple given by Eq. (1):

$$An^{3+} + 3e^- = An \qquad (\text{or } Ln^{3+} + 3e^- = Ln) \tag{1}$$

The cathodic peak shifted slightly in the negative direction with the increase of potential scanning rate, while the anodic

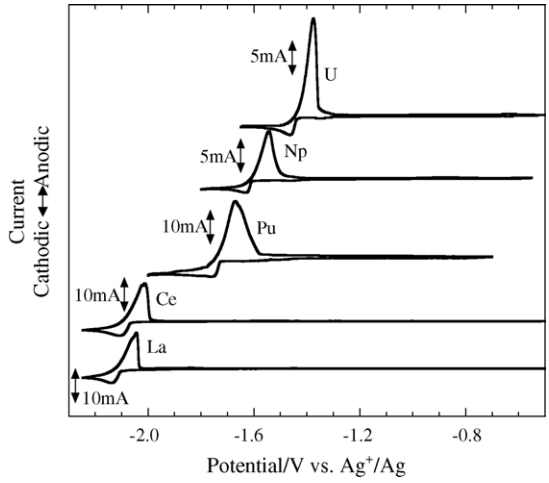

Fig. 1. Cyclic voltammograms for the redox reactions of the U^{3+}/U, Np^{3+}/Np, Pu^{3+}/Pu, La^{3+}/La and Ce^{3+}/Ce couples at Mo electrodes at 773 K.

Table 1
Standard potentials, $E^{0'}$, for the U^{3+}/U, Pu^{3+}/Pu, Np^{3+}/Np, La^{3+}/La and Ce^{3+}/Ce couples vs. Ag^+/Ag (1 wt.%) or Cl_2/Cl^- reference electrodes and standard free energies of formation for metal chlorides, $G^0_{fMCl_3}$, in LiCl–KCl eutectic melts at 773 K

Couple	$E^{0'}_{M^{3+}/M}$ (V vs. Ag^+/Ag)	$E^{0'}_{M^{3+}/M}$ (V vs. Cl_2/Cl^-)	$G^0_{fMCl_3}$ (kJ mol^{-1})
U^{3+}/U	−1.2478	−2.4533	−710.12
Pu^{3+}/Pu	−1.506	−2.711	−784.7
Np^{3+}/Np	−1.4845	−2.6900	−778.63
La^{3+}/La	−1.9310	−3.1364	−907.85
Ce^{3+}/Ce	−2.0260	−3.2314	−935.35

peak stayed almost constant. These characteristics indicate that the influence of overpotential such as crystallization on the deposition of An or Ln metal cannot be neglected, though the anodic reaction is rapid [14]. Therefore, potentiometric methods were applied in order to obtain accurate values of the redox potentials of the An^{3+}/An and Ln^{3+}/Ln couples. The formal potentials of the An^{3+}/An and Ln^{3+}/Ln couples, $E^{0'}_{An^{3+}/An}$ or $E^{0'}_{Ln^{3+}/Ln}$, in the LiCl–KCl melts obtained by the measurement of electromotive force are shown in Table 1 [15,16]. The $E^{0'}_{An^{3+}/An}$ and $E^{0'}_{Ln^{3+}/Ln}$ values were obtained by extrapolation of the linear E versus $\ln c_{AnCl_3}$ or $\ln c_{LnCl}$ plot to the intercept. These are accordance with the reported values [17,18]. The formal potentials versus the Ag^+/Ag electrode are expressed by Eqs. (2)–(6):

$$E^{0'}_{U^{3+}/U} = -1.8647 + 0.000798 \times T(\text{V versus } Ag^+/Ag) \quad (2)$$

$$E^{0'}_{Np^{3+}/Np} = -2.0298 + 0.000706 \times T(\text{V versus } Ag^+/Ag) \quad (3)$$

$$E^{0'}_{Pu^{3+}/Pu} = -2.232 + 0.00094 \times T(\text{V versus } Ag^+/Ag) \quad (4)$$

$$E^{0'}_{La^{3+}/La} = -2.5742 + 0.001001 \times T(\text{V versus } Ag^+/Ag) \quad (5)$$

$$E^{0'}_{Ce^{3+}/Ce} = -2.5549 + 0.000851 \times T(\text{V versus } Ag^+/Ag) \quad (6)$$

where T is in K.

By using the data of Yang and Hudson at low-AgCl concentrations in the LiCl–KCl eutectic melt [19], the following equation is obtained for potential of the reference electrode, $E_{Ag^+/Ag}$, relative to the Cl_2/Cl^- couple:

$$E_{Ag^+/Ag} = -1.0659 - 0.0001805 \times T(\text{V versus } Cl_2/Cl^-) \quad (7)$$

Therefore, the formal potentials of the An^{3+}/An and Ln^{3+}/Ln couples versus the Cl_2/Cl^- reference electrode, $E^{0'}_{An^{3+}/An}$ (Cl_2/Cl^-) or $E^{0'}_{Ln^{3+}/Ln}$ (Cl_2/Cl^-), can be represented by using Eqs. (8)–(12):

$$E^{0'}_{U^{3+}/U}(Cl_2/Cl^-) = -2.9306 + 0.000618 \times T(\text{V versus } Cl_2/Cl^-) \quad (8)$$

$$E^{0'}_{Np^{3+}/Np}(Cl_2/Cl^-) = -3.0957 + 0.000521 \times T(\text{V versus } Cl_2/Cl^-) \quad (9)$$

$$E^{0'}_{Pu^{3+}/Pu}(Cl^2/Cl^-) = -3.298 + 0.00076 \times T(\text{V versus } Cl_2/Cl^-) \quad (10)$$

$$E^{0'}_{La^{3+}/La}(Cl_2/Cl^-) = -3.6401 + 0.000821 \times T(\text{V versus } Cl_2/Cl^-) \quad (11)$$

$$E^{0'}_{Ce^{3+}/Ce}(Cl_2/Cl^-) = -3.6208 + 0.000671 \times T(\text{V versus } Cl_2/Cl^-) \quad (12)$$

The Gibbs free energies, $G^0_{fAnCl_3}$ and $G^0_{fLnCl_3}$, of formation of $AnCl_3$ and $LnCl_3$ in the LiCl–KCl melt are calculated from the $E^{0'}_{An^{3+}/An}$ (Cl_2/Cl^-) and $E^{0'}_{Ln^{3+}/Ln}$ (Cl_2/Cl^-) values by using the following relation:

$$G^0_{fAnCl_3} = nFE^{0'}_{An^{3+}/An}(Cl_2/Cl^-)\{\text{or } G^0_{fLnCl_3} = nFE^{0'}_{Ln^{3+}/Ln}(Cl_2/Cl^-)\} \quad (13)$$

3.2. The redox reaction of the U^{3+}/U, Np^{3+}/Np and Pu^{3+}/Pu couples at the liquid Cd and Bi electrodes

Cyclic voltammograms for the redox reactions of the U^{3+}/U, Np^{3+}/Np and Pu^{3+}/Pu couples at the liquid Cd electrodes are shown in Fig. 2. The solid lines show the voltammogram for the redox reaction at the interface between the liquid Cd phase and the LiCl–KCl eutectic melt containing 0.55 wt.% UCl_3 (0.00088 mol fraction), 0.465 wt.% $NpCl_3$ (0.00070 mol fraction) and 0.87 wt.% $PuCl_3$ (0.0014 mol fraction), respectively, at 723 K. The broken lines show the voltammogram obtained at the interface between the liquid Cd phase and the LiCl–KCl melt in the absence of UCl_3, $NpCl_3$ and $PuCl_3$. The anodic current, which corresponds to the oxidation of Cd ($Cd = Cd^{2+} + 2e^-$), was observed, when the potential of the liquid Cd electrode was scanned

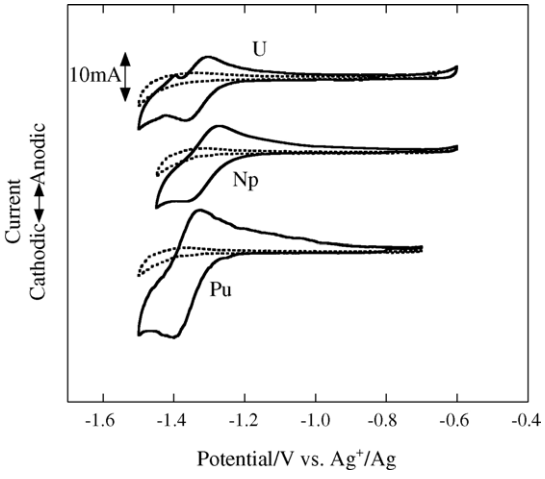

Fig. 2. Cyclic voltammograms for the redox reactions of the U^{3+}/U, Np^{3+}/Np and Pu^{3+}/Pu couples at liquid Cd electrodes at 773 K. Working electrode: Cd (area: 0.605 cm^2). Scan rate: 0.01 V s^{-1}.

to more positive potential than −0.60 V. On the other hand, the final descent was observed at around −1.45 V, which corresponds to the reduction of Li^+ ($Li^+ + e^- = Li$) [20]. There are a couple of cathodic and anodic peaks in each solid line. Irrespective of potential scanning rate, the cathodic and anodic peak potentials remained almost constant. The number of the transferred electron, n, was calculated to be 2.7–3.0 from the relation between the cathodic peak potential, E_p^c, and the cathodic half-peak potential, $E_{p/2}^c$, of the cyclic voltammograms at potential scanning rate between 0.010 and 0.200 V s^{-1} ($E_p^c - E_{p/2}^c = -2.2RT/nF$). The cathodic current peaks were proportional to the concentrations of $AnCl_3$. The above characteristics indicate that the redox reactions of the An^{3+}/An couples at the Cd electrodes are almost reversible under the experimental conditions. By considering the relation between the half wave potential, $E_{1/2}$, and E_p^c and that between $E_{1/2}$ and $E_{p/2}^c$, $E_{1/2}$ can be evaluated. The potential differences between the redox potentials of the An^{3+}/An couple at the Mo electrode and those at the liquid Cd electrode are shown in Table 2.

The potential differences between the redox reactions of the An^{3+}/An couple at the Mo electrode and those at the liquid Cd electrode were independent of the concentration of $AnCl_3$ in the LiCl–KCl melt. Therefore, the difference between the redox potential of the An^{3+}/An couple at the liquid Cd electrode and that at the Mo electrode might be attributable to a lowering of activity of An in the Cd phase [21–23]. Because the activity of An in the Cd phase depends on the dissolved condition and the concentration of An in the Cd phase, the potential difference can be explained by assuming the formation of $AnCd_n$ which is the most stable intermetallic compound among the An–Cd system. $AnCd_n$ will be formed in the liquid Cd phase as Eq. (14):

$$An + nCd = AnCd_n \tag{14}$$

Here, $AnCd_{11}$ is most stable in each case at 773 K. On the other hand, the redox potential of the An^{3+}/An couple at the solid electrode versus the Ag^+/Ag reference electrode, $E_{An^{3+}/An}$, is expressed as follows:

$$E_{An^{3+}/An} = E^{0'}_{An^{3+}/An} + \frac{RT}{3F} \ln \frac{[An^{3+}]}{[An]} \tag{15}$$

Accordingly, the redox potential of the An^{3+}/An couple at the liquid Cd electrode, $E_{An^{3+}/An-Cd}$, is described as Eq. (16) by using the activity coefficient, γ, and the concentration, c (in mole fraction):

$$E_{An^{3+}/An-Cd} = E_{An\ ^{3+}/An} - \frac{G^0_{AnCd_n}}{3F} + \frac{nRT}{3F} \ln \gamma_{Cd,Metal} c_{Cd,\ Metal} - \frac{RT}{3F} \ln \gamma_{AnCd_n,Metal} c_{AnCd_n,Metal} \tag{16}$$

where $G^0_{AnCd_n}$ is the standard free energy of formation of $AnCd_n$. Therefore, the potential difference, ΔE, between $E_{An^{3+}/An-Cd}$ and $E_{An3+/An}$ is represented as Eq. (17):

$$\Delta E = -\frac{G^0_{AnCd_n}}{3F} + \frac{nRT}{3F} \ln \gamma_{Cd,Metal} c_{Cd,Metal} - \frac{RT}{3F} \ln \gamma_{AnCd_n,Metal} c_{AnCd_n,Metal} \tag{17}$$

Since the solubilities of An in the Cd phase at the temperature range from 723 to 823 K are very low, it seems reasonable to suppose that $\gamma_{AnCd_n,Metal}$ and $c_{AnCd_n,Metal}$ are close to unity. Because Cd is the principal constituent of the liquid metal phase, $\gamma_{Cd,Metal}$ will be also close to unity. If one takes into

Table 2
Standard redox potentials of the An^{3+}/An couple at liquid Cd or Bi electrode ($E^{0'}_{An^{3+}/An-Cd}$ or $E^{0'}_{An^{3+}/An-Bi}$), potential differences between the standard potential at Mo electrode and $E^{0'}_{An^{3+}/An-Cd}$ or $E^{0'}_{An^{3+}/An-Bi}$ (ΔE_{Cd} or ΔE_{Bi}) and standard free energies of formation for metallic alloy (G^0_f) at 773 K

Species	Working electrode	$E^{0'}_{An^{3+}/An-Cd}$ or $E^{0'}_{An^{3+}/An-Bi}$ (V vs. Ag^+/Ag)	ΔE_{Cd} or ΔE_{Bi} (V)	G^0_f (kJ mol^{-1})
U	Cd	−1.310	−0.062	−17.9
	Bi	−0.970	0.278	80.5
Np	Cd	−1.345	0.140	40.5
	Bi	−1.066	0.419	121
Pu	Cd	−1.376	0.315	91.2
	Bi	−1.080	0.572	165.6

account the above assumptions, Eq. (17) can be simplified to Eq. (18):

$$\Delta E = -\frac{G^0_{\mathrm{AnCd}_n}}{3F} + \frac{2RT}{F} \ln c_{\mathrm{Cd,Metal}} \quad (18)$$

By considering reported values of $G^0_{\mathrm{AnCd}_n}$ and $c_{\mathrm{An,Metal}}$, the estimated ΔE values are almost in agreement with the experimental values mentioned before. This result suggests that the potential shift almost corresponds to the free energy of formation of the intermetallic compound, AnCd_n, in the liquid Cd phase:

In the case of the Bi liquid electrode, the redox reactions of the $\mathrm{An^{3+}/An}$ couples can be analyzed in a similar manner as above. The potential differences between the redox potentials of the $\mathrm{An^{3+}/An}$ couples at the liquid Bi electrode and those at the Mo electrode are shown in Table 2 and are attributable to a lowering of activity of An in the Bi phase [23,24]. Since the activity of An in the Bi phase depends on the dissolved condition and the concentration of An in the Bi phase, the potential difference could be explained by forming of AnBi_n as Eq. (19). In the present condition, $\mathrm{AnBi_2}$ will be formed in the liquid Bi phase:

$$\mathrm{An} + n\mathrm{Bi} = \mathrm{AnBi}_n \quad (19)$$

The potential difference, ΔE, between $E_{\mathrm{An^{3+}/An-Bi}}$ and $E_{\mathrm{An^{3+}/An}}$ is represented as Eq. (20):

$$\Delta E = -\frac{G^0_{\mathrm{AnBi}_n}}{3F} + \frac{nRT}{3F} \ln \gamma_{\mathrm{Bi,Metal}} c_{\mathrm{Bi,Metal}} - \frac{RT}{3F} \ln \gamma_{\mathrm{AnBi}_n,\mathrm{Metal}} c_{\mathrm{AnBi}_n,\mathrm{Metal}} \quad (20)$$

In analogy with the electrode reaction of An at the Cd electrode, it seems to be that $\gamma_{\mathrm{Bi,Metal}}$, $\gamma_{\mathrm{AnBi_n,Metal}}$ and $c_{\mathrm{AnBi_n,Metal}}$ are close to unity locally. Therefore, Eq. (20) can be simplified to Eq. (21):

$$\Delta E = -\frac{G^0_{\mathrm{AnBi}_n}}{3F} + \frac{2RT}{F} \ln c_{\mathrm{Bi,Metal}} \quad (21)$$

By considering reported values of $G^0_{\mathrm{AnBi}_n}$ and $c_{\mathrm{Bi,Metal}}$, the estimated ΔE values are also in good agreement with the experimental values [15,16,25]. This result suggests that the potential shift almost corresponds to the free energy of formation of the intermetallic compound, AnBi_n (Fig. 3).

3.3. Voltammetric studies on actinide mononitride

Fig. 4 shows cyclic voltammograms for the redox behaviors of UN, NpN and PuN in the LiCl–KCl eutectic salt containing with 0.30 wt.% $\mathrm{UCl_3}$, 0.53 wt.% $\mathrm{NpCl_3}$ and 0.54 wt.% $\mathrm{PuCl_3}$, respectively, at 773 K. The anodic current, which was caused from the reaction represented by the following Eq. (22), was observed in each voltammogram:

$$\mathrm{AnN} = \mathrm{An^{3+}} + 3\mathrm{e^-} + 1/2\mathrm{N_2} \quad (22)$$

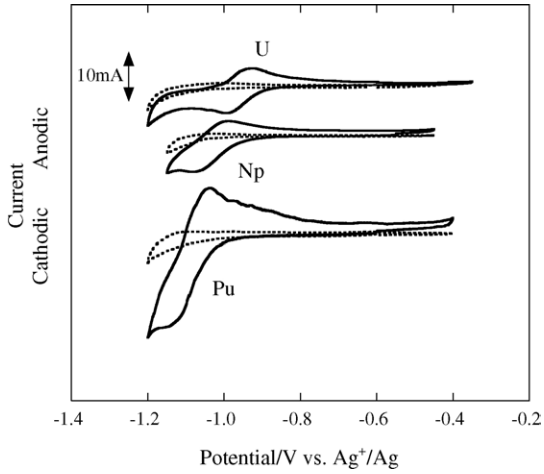

Fig. 3. Cyclic voltammograms for the redox reactions of the U^{3+}/U, Np^{3+}/Np and Pu^{3+}/Pu couples at liquid Bi electrodes at 773 K. Working electrode: Bi (area: 0.605 $\mathrm{cm^2}$). Scan rate: 0.01 $\mathrm{V\,s^{-1}}$.

The cathodic currents observed in the reverse potential sweep of the voltammograms were less than the anodic currents because the N_2 gas generated with the anodic dissolution of their nitrides in the salt was escaped from the salts. The reaction (22) seems to be slow and a rate-determining step, since the current did not increase in proportion to square root of the potential scanning rate and the cathodic peak is shifted to the negative direction with increasing the potential scanning rate.

The redox potentials of AnN, $E_{\mathrm{AnN-Ag^+/Ag}}$, is described as Eq. (23) by the same procedure as in the previous work [8]:

$$E_{\mathrm{AnN-Ag^+/Ag}} = E^0_{\mathrm{An^{3+}}} - \frac{G^0_{\mathrm{AnN}}}{3F} + \frac{(RT)}{(3F)} \ln \gamma_{\mathrm{An^{3+}}} c_{\mathrm{An^{3+}}} + \frac{(RT)}{(6F)} \ln p_{\mathrm{N_2}} \quad (23)$$

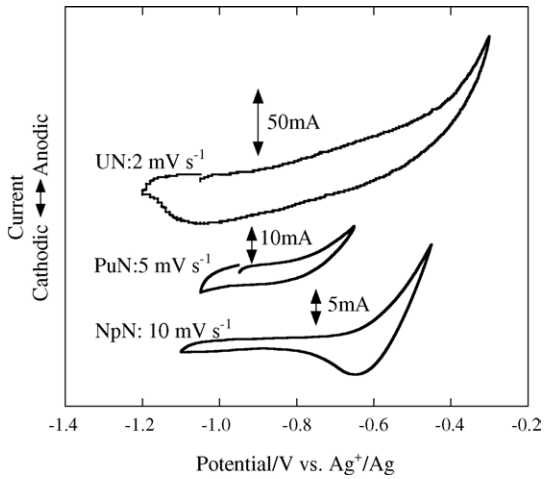

Fig. 4. Cyclic voltammograms for the dissolutions of UN, NpN and PuN at 773 K.

The standard free energies of formation, G^0_{AnN}, of UN, NpN and PuN at 773 K are −225.90, −226.41 and −232.20 kJ mol^{-1} [26], respectively. The concentrations of UCl_3, $NpCl_3$ and $PuCl_3$ in the melts were 0.30 wt.% (0.049 mol.%), 0.53 wt.% (0.086 mol.%) and 0.54 wt.% (0.087 mol.%), respectively. Therefore, the equilibrium potentials at 773 K derived from Eq. (23) are expressed as follows [8–10]:

$$E_{UN-Ag^+/Ag} = -0.637 + 0.0111 \times \ln p_{N_2} \quad (24)$$

$$E_{NpN-Ag^+/Ag} = -0.729 + 0.0111 \times \ln p_{N_2} \quad (25)$$

$$E_{PuN-Ag^+/Ag} = -0.864 + 0.0111 \times \ln p_{N_2} \quad (26)$$

The equilibrium potentials of UN, NpN and PuN at 773 K obtained by the electromotive force measurements were -0.710 ± 0.010, -0.773 ± 0.005 and -0.880 ± 0.005 V, respectively. These values are comparable with the equilibrium potentials estimated by substituting the p_{N2} values ranging from 0.001 to 0.2 atm in the cell atmosphere in Eqs. (24)–(26).

The anodic current increased drastically around −0.4 V in the voltammogram for the dissolution of UN. Kobayashi et al. reported this anodic reaction was attributable to the formation of UNCl and U_2N_3 [27]. However, the authors reported that the redox reaction of the U^{4+}/U^{3+} couple was overlapped with the dissolution of UN [10]. Consequently, we proposed the mechanism that U^{3+} was oxidized to U^{4+} at the anode, U^{4+} was reduced to U^{3+} at the cathode, and UNCl was formed directly from UN described as Eq. (27):

$$UN = UN^+ + e^- \qquad \{\text{and } UN^+ + Cl^- = UNCl\} \quad (27)$$

Here, UN^+ is considered to be formed by oxidation of UN, since U behaves like a trivalent ion in UN. The UNCl formed was precipitated, and the circulation current, which occurred by the reduction of U^{4+} to U^{3+} at the cathode and the oxidation of U^{3+} to U^{4+} at the anode at the same time, flowed in the cell system. Accordingly, the electrolysis efficiency will be lowered in the presence of UN in the cell. Taking into account the above information on the electrolysis, the electrolysis using a mixture of various nitrides in the presence of UN as an anode by applying more negative potential than −0.4 V should be performed in order to diminish the loss in the recovery process.

The redox potential of NpN was observed at more positive than that of PuN by about 0.15 V and at more negative than that of UN by about 0.10 V. Accordingly, it would be difficult to separate a mixture of plural nitrides into each component by anodic dissolution of the nitrides, since the rate of anodic dissolution of nitrides is slow and the redox potentials of NpN, UN and PuN lie closely together. In order to establish the electrochemical refining of nitride fuels, it is necessary to investigate not only static parameters such as standard redox potential and activity coefficient but also kinetic parameters such as rate constant and diffusion coefficient.

4. Conclusion

The electrode reactions of the An^{3+}/An couples at various working electrodes in the LiCl–KCl eutectic melt were elucidated electrochemically. The redox potentials of the An^{3+}/An couples at the liquid metal electrodes were shifted to the positive direction in comparison with those at the Mo electrodes. The potential shifts almost corresponded to the free energies of formation of the intermetallic compounds in the liquid metal phases. UN, NpN and PuN were dissolved as U^{3+}, Np^{3+} and Pu^{3+} with the generation of N_2 gas in the LiCl–KCl eutectic melt at 773 K. If the applied potential on the surface of UN was more positive than −0.4 V, U^{3+} was oxidized to U^{4+} at the anode, U^{4+} was reduced to U^{3+} at the cathode, and UNCl was formed directly from UN. Then, the electrolytic efficiency was lowered in this case.

Acknowledgements

The authors are grateful to Mr. T. Iwai of JAERI and Drs. T. Fujii and A. Uehara of Kyoto University for their interest and useful suggestions.

References

[1] T. Mukaiyama, H. Takano, T. Ogawa, T. Takizuka, M. Mizumoto, Prog. Nucl. Energy 40 (2002) 403–413.
[2] H. Brank, Materials Science and Technology, Nuclear Materials, vol. 10A, VCH, Weinheim, 1994.
[3] Hj. Matzke, Science of Advanced LMFBR Fuels, North-Holland, Amsterdam, 1986.
[4] T. Mukaiyama, M. Kubota, T. Takizuka, T. Ogawa, M. Mizumoto, H. Yoshida, Proceedings of the International Conference on Evaluation of Emerging Nuclear Fuel Cycle Systems “GLOBAL’95”, vol. 1, Versailles, France, 1995, pp. 110–117.
[5] J.E. Till, E.S. Bomar, L.E. Morse, V.J. Tennery, Nucl. Technol. 37 (1978) 328–339.
[6] Y. Arai, T. Iwai, K. Nakajima, Y. Suzuki, Proceeding of the International Conference on Future Nuclear Systems “GLOBAL’97”, vol. 1, Yokohama, Japan, October 5–10, 1997, pp. 664–669.
[7] T. Ogawa, M. Akabori, Y. Suzuki, F. Kobayashi, T. Osugi, T. Mukaiyama, Proceedings of the International Conference on Future Nuclear Systems “GLOBAL’97”, vol. 1, Yokohama, Japan, October 5-10, 1997, pp. 812–815.
[8] O. Shirai, T. Iwai, K. Shiozawa, Y. Suzuki, Y. Sakamura, T. Inoue, J. Nucl. Mater. 277 (2000) 226–230.
[9] O. Shirai, M. Iizuka, T. Iwai, Y. Suzuki, Y. Arai, J. Nucl. Sci. Technol. 37 (2000) 676–681.
[10] O. Shirai, K. Uozumi, T. Iwai, Y. Arai, J. Nucl. Sci. Technol. 3 (2000) 745–748 (Supplement).
[11] J.P. Ackerman, Ind. Eng. Chem. Res. 30 (1991) 141–145.
[12] M. Iizuka, T. Koyama, N. Kondo, R. Fujita, H. Tanaka, J. Nucl. Mater. 247 (1997) 83–190.
[13] O. Shirai, M. Iizuka, T. Iwai, Y. Suzuki, Y. Arai, J. Electroanal. Chem. 490 (2000) 31–36.
[14] T. Berzins, P. Delahay, J. Am. Chem. Soc. 75 (1953) 555–559.
[15] O. Shirai, K. Uozumi, T. Iwai, Y. Arai, Anal. Sci. 17 (2000) i959–i962 (Supplement).
[16] O. Shirai, K. Uozumi, T. Iwai, Y. Arai, J. Appl. Electrochem. 34 (2000) 323–330.

[17] Y. Sakamura, T. Hijikata, K. Kinoshita, T. Inoue, T.S. Storvick, C.L. Krueger, J.J. Roy, D.L. Grimmett, S.P. Fusselman, R.L. Gay, J. Alloys Comp. 271–273 (1998) 592–596.
[18] S.P. Fusselman, J.J. Roy, D.L. Grimmett, L.F. Grantham, C.L. Krueger, C.R. Nabelek, T.S. Storvick, T. Inoue, T. Hijikata, K. Kinoshita, Y. Sakamura, K. Uozumi, T. Kawai, N. Takahashi, J. Electrochem. Soc. 146 (1999) 2573–2580.
[19] L. Yang, R.G. Hudson, J. Electrochem. Soc. 106 (1959) 986–990.
[20] M.A. Lewis, T.R. Johnson, J. Electrochem. Soc. 137 (1990) 1414–1418.
[21] I. Johnson, M.G. Chasanov, R.M. Yonco, Trans. Met. Soc. AIME 233 (1965) 1408–1414.
[22] D.E. Etter, et al., Trans. Met. Soc. AIME 233 (1965) 2011–2013.
[23] P. Chiotti, V.V. Akhachinskij, I. Ansara, M.H. Rand, The Chemical Thermodynamics of Actinide Elements and Compounds. Part 5. The Actinide Binary Alloys, vol. 221, International Atomic Energy Agency, Vienna, 1981.
[24] V.A. Lebedev, L.G. Babikov, S.K. Vavilov, I.F. Nichkov, S.P. Raspopin, O.V. Skiba, Sov. J. At. Energy 27 (1969) 748–750.
[25] O. Shirai, M. Iizuka, T. Iwai, Y. Arai, Anal. Sci. 17 (2001) 51–57.
[26] I. Bari, Thermochemical Data of Pure Substances, 3rd ed., VCH, Weinheim, 1995.
[27] F. Kobayashi, T. Ogawa, Y. Okamoto, M. Akabori, Y. Kato, J. Am. Ceram. Soc. 78 (1995) 2279–2282.